
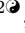



Uncoupling the roles of firing rates and spike bursts in shaping the GPe-STN beta band oscillations

Jyotika Bahuguna^{1*}, Ajith Sahasranamam², Arvind Kumar^{3*},

1 Aix Marseille University, Institute for Systems Neuroscience, Marseille, France

2 Ongil Pvt Ltd, Singapore

3 Department of Computational Science and Technology, School of Electrical Engineering and Computer Science, KTH Royal Institute of Technology, Sweden

 These authors contributed equally to this work.

* arv Kumar@kth.se, jyotika.bahuguna@gmail.com

Abstract

The STN-GPe circuit is integral to generation and modulation of β oscillations in basal ganglia. However, how do their firing rates and spike bursting affect the oscillations is unclear. In order to uncouple their effects, we performed spiking neural network simulations of STN-GPe using a neuron model, where firing rates and spike bursting can be independently controlled. We find that the presence of oscillations are reliant on STN firing rates but not on GPe rates. The effect of GPe/STN bursting is state-dependent i.e only in network states on the border of oscillatory and non-oscillatory regime, an increase in GPe bursting strengthens the oscillations whereas an equivalent proportion of STN bursting suppresses them. We propose that these incursions into oscillatory and back to non-oscillatory state constitutes what we know as “ β bursts”. During PD, however, the network shifts deeper into oscillatory regime where this mechanism fails leading to runaway oscillations.

Introduction

Parkinson’s disease (PD) is a progressive neurodegenerative brain disease caused by the depletion of dopamine neurons in the substantia nigra pars compacta (SNc). PD patients suffer from a host of cognitive and motor impairments, the behavioral symptoms of which are accompanied by various changes in the neuronal activity in Basal Ganglia (BG): e.g, increased firing rate of D2 type dopamine receptors expressing striatal neurons [1–3]; increased bursting in striatum, globus pallidus externa (GPe), globus pallidus interna (GPi) and subthalamic nuclei (STN) [2] and increased synchrony in all BG nuclei [4] including striatum [5], GPe [6, 7], STN [3, 8, 9] and GPi/SNr [6, 10, 11]. Besides these changes in neuronal activity, at the population level, there is an increase in the power and duration of β band oscillations (15–30 Hz) in local field potential (LFP) recorded from the basal ganglia of PD patients [8, 11–13]. The β band oscillations are mainly correlated with motor deficits such as rest tremor and akinesia [3, 8, 14, 15] and, suppression of these oscillations, for example, by deep brain stimulation (DBS) ameliorates motor symptoms of PD. Therefore, there is a great interest in understanding the mechanisms underlying the origin of β band oscillations which are still not well understood [16]. For instance, it is unclear whether the oscillations are imposed by cortical inputs [17–19] or they are generated within the BG,

either in striatum [20], in pallidostriatal circuit [21] or the GPe-STN circuit [2,16,22–28]. Several experimental results indicate that GPe-STN network plays an integral role in generating and modulating these oscillations [8,11,12,29] and their stimulation have been shown to affect (disrupt/modulate) oscillations [2,30,31].

From a dynamical systems perspective, interaction between excitatory and inhibitory neuronal population form the necessary substrate for oscillations where an imbalance of timing and/or strength of effective excitation and inhibition leads to population oscillations [32]. Several excitatory and inhibitory loops can be identified in the BG which may underlie the emergence of β band oscillations among which GPe-STN circuit has emerged as a primary candidate. In both firing rate-based and spiking neuronal network models, an increase in the coupling between STN and GPe is sufficient to induce strong persistent oscillations [23,26,27]. However, the oscillations may also be created if effective excitatory input to STN neurons (from the cortex) or effective inhibitory input to GPe neurons (from the striatum) is increased [24,28]. Besides, the GPe-STN network, the imbalance of the direct (effectively excitatory) and hyper-direct (effectively inhibitory) pathways of the BG can also cause oscillations [33]. These computational models not only suggest possible mechanisms underlying the β oscillations but also provide explanations for the altered synaptic connectivity within the BG and how increased firing rates in the striatal neuron projecting to the GPe [1] can lead to pathological oscillations.

The β band oscillations are also accompanied by an increase in spike bursting along with the firing rate changes. In MPTP models of non-human primates, the proportion of bursty spikes in STN and GPe is significantly higher in animals with PD than the healthy animals [2,34]. Increased spike bursting in GPe and STN is also observed in 6-OHDA treated rodents [35,36]. But it remains unclear how increased spike bursting affects the duration and power of β band oscillations.

However, it should be noted neurons in the STN-GPe network show spike bursting even in healthy conditions [2,34]. Therefore, it is important to understand whether the bursting spikes and the pathological oscillations share a causal relationship and if this is the case, then why spike bursts are also observed in healthy states [2,34].

To understand the role of spike bursting in shaping the beta oscillations here, we investigated the effect of firing rates and patterns on the presence of oscillations using a computational model of the STN-GPe network. Usually, the average firing rate is tightly coupled to spike bursting and it is not easy to disentangle the effect of these two variables independently. To solve this we used the State-dependent Stochastic Bursting Neuron Model (SSBN) model [37], which allowed us to vary firing rate and firing pattern (spike bursting) of the neuron independently and hence uncouple the effects of firing rate and bursting on the β band oscillations.

Using the model, we found that the average firing rate of STN neurons is predictive of oscillation but surprisingly, the average firing rate of GPe neurons was not. The effect of GPe and STN bursting on STN-GPe oscillations was however, state dependent. When the network exhibited strong oscillations or aperiodic activity, spike bursting in STN and GPe had no effect on the global state of network activity. However, in the regime at the border of oscillatory and non-oscillatory states, an increase in the fraction of bursting neurons in GPe, enhanced oscillations. By contrast, small to moderate fraction of bursting neurons in STN quenched the oscillations whereas when most of the STN neurons were bursting, network re-exhibited strong oscillations. Taken together, these results for the first time separate the roles of firing rates and bursting and shows how spike bursting in the STN and GPe can either enhance or suppress the β band oscillations, depending on the network activity state. Finally, our results revealed that STN and GPe may play a qualitatively different role in shaping of the dynamics of beta band oscillations. These insights suggest new means quench the pathological oscillations.

Materials and methods

Neuron model

In the existing reduced neuron models (e.g. leaky-integrate-fire neuron), to achieve changes in the firing patterns, the sub-threshold dynamics of the neuron model needs to be altered. However, when a neuron model is modified to exhibit spike bursting, its input-output firing rate relationship ($f - I$ curve) is also altered. That is, spike bursting and neuron firing rate are coupled and prevent the comparison with non-bursting neuron with the same firing rate. However, to isolate the effect of changes in the firing patterns on the network dynamics, the $f - I$ curve of the neuron and its firing pattern need to be independently controlled. To achieve this, we use the State-dependent Stochastic Bursting Neuron (SSBN) [37]. The subthreshold membrane potential dynamics of the SSBN model is same as that of the Leaky Integrate and Fire (LIF) neuron:

$$\tau_m \dot{V}_m = -V_m + I_{syn}$$

where, τ_m is the membrane time constant, V_m is the membrane potential and I_{syn} is the total synaptic current to the neuron. The spike generation mechanism of SSBN is stochastic. On reaching the spiking threshold V_{th} , the SSBN generates a burst of b spikes with a probability of $1/b$ every time $V_m \geq V_{th}$. This allows us to vary the size of spike burst without affecting the spike rate and the input output neuron transfer function of the neuron (in Figure Supplement ??). The inter-spike-interval within the burst is constant ($2ms$). More details about this neuron model can be found at [37]. All the neurons in the STN and GPe were modelled as SSBNs. The neuron parameters used are consistent with the STN-GPe network used in a recent work by [28] and are listed in **Table. 1**. We used the same neuron parameters for STN and GPe neurons, however the two neuron types received different amount of external inputs as we explored network state space for different external inputs to the GPe and STN.

Table 1. Neuron parameters as used in [28].

Parameter	Value	Description
C_m	$200pF$	Membrane capacitance
τ_m	$20ms$	Membrane Time Constant
V_{th}	$-54mV$	Firing threshold
V_{reset}	$-70mV$	Reset potential
τ_{ref}	$5ms$	Refractory period
B_{isi}	$2ms$	Inter-spike interval within a spike burst
B	1 or 4	Number of spikes in a burst
τ_{exc}	$5ms$	Excitatory synaptic time constant
τ_{inh}	$10ms$	Inhibitory synaptic time constant
g_L	$10nS$	Leak conductance
E_{ex}	$0mV$	Reversal potential (excitatory)
E_{in}	$-80.0mV$	Reversal potential (inhibitory)

Synapse model

Synapses were modelled as a transient change in conductance. Each spike elicited an alpha-function shaped change in the post-synaptic conductance. The reversal potential

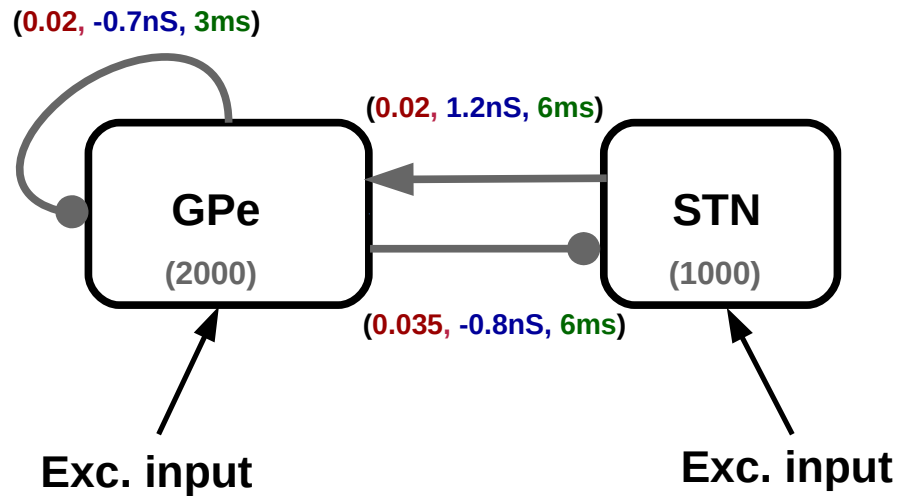


Fig 1. Schematic of the STN-GPe network. The connection probability, synaptic strength and delay for each connection is shown in red, blue and green, respectively. The number in parentheses (1000, 2000) represent the number of neurons in STN and GPe, respectively. The connection with arrowhead are excitatory and those with filled circle are inhibitory. The F-I curves for the neuron model with different burst lengths is plotted in Supplement Figure ???. The inter spike interval within the burst is kept constant (2ms).

determined the whether the synapse was excitatory or inhibitory. The peak conductance of each type of synapse is provided in the Figure. 1 and **Table 2** and the excitatory and inhibitory time constants are shown in **Table 1**. For further details on dynamics, refer to "iaf_cond_alpha" neuron model in NEST [38].

STN-GPe network model

The network model consisted of 2000 inhibitory (corresponding to the GPe population) and 1000 excitatory (corresponding to the STN population) neurons. The neurons were connected in a random manner with fixed connection probabilities. The connection strength, connection probability and synaptic delays were identical to the one used in the model by Mirzaei11220 and are shown in Fig. 1 and Table 2.

We investigated the oscillation dynamics of the STN-GPe network in two conditions:

- Condition A: To characterize the effect of firing rates on β band oscillations we studied the network when all the neurons were non-bursting type. For these simulations we set $B = 1$ for all the neurons.
- Condition B: To characterize the effect of spike bursting on β band oscillations we used networks in which a fraction of STN and/or GPe neurons were bursting type. The fraction of bursting neurons in the two populations was varied systematically from 0 to 1. For these simulation we set the spike burst length $B = 4$ for the bursting neurons and $B = 1$ for the non-bursting (or regular spiking neurons).

Table 2. Network parameters as used in [28]

Parameter	Value	Description
$\epsilon_{gpe-gpe}$	0.02	GPe to GPe connectivity
$\epsilon_{gpe-stn}$	0.035	GPe to STN connectivity
$\epsilon_{stn-gpe}$	0.02	STN to GPe connectivity
$J_{gpe-gpe}$	$-0.7nS$	GPe to GPe synaptic strength
$J_{gpe-stn}$	$-0.8nS$	GPe to STN synaptic strength
$J_{stn-gpe}$	$1.2nS$	STN to GPe synaptic strength
$\tau_{gpe-gpe}$	$3ms$	GPe to GPe synaptic delay
$\tau_{gpe-stn}$	$6ms$	GPe to STN synaptic delay
$\tau_{stn-gpe}$	$6ms$	STN to GPe synaptic delay

Input

All neurons in the STN and GPe received external excitatory input which was modelled as uncorrelated Poisson spike trains. This input was tuned to match the range of firing rates of the STN and GPe observed in *in vivo* data during healthy and Parkinsonian conditions [12, 28, 36].

To characterize the role of firing rates simulations (condition A) we systematically varied the rate of Poisson spike trains independently for the STN and GPe neurons. For each parameter set we performed at least 5 trials with different random seeds.

Data Analysis

Spectrum of the population activity

To estimate the spectrum of the network activity we binned (bin width = 5 ms) the spiking activity of all the STN or GPe neurons to obtain the population activity (S). We subtracted the mean and estimated the spectrum (P) using the fast Fourier transform (frequency resolution = 5 Hz). To estimate spectral entropy (see below) we measured the P for the whole duration of simulations (7500 ms). To estimate the time-resolved spectrum we measured P for sliding windows (window size = 200ms; overlap = 50ms)

Spectral Entropy

To quantify how oscillatory the network activity was, we computed the spectral entropy H_S , which is a measure of dispersion of spectral energy of a signal [37, 39].

$$H_S = \frac{-\sum_k P_k \log P_k}{\log N}$$

where P_k is the spectral power at frequency k and N is the total number of frequency bins considered. To estimate spectral entropy we normalized P_k such that $\sum_k P_k = 1$. The spectral power was calculated in the β frequency range, i.e., 10-35 Hz.

An aperiodic signal (e.g. white noise) for which the spectral power is uniformly distributed over the whole frequency range, has $H_S = 1$. By contrast, periodic signals that exhibit a peak in their spectrum (e.g. in the β band) have lower values of H_S . In an extreme case, for a single frequency sinusoidal signal $H_S = 0$. Thus, H_S varies between 0 and 1.

Duration and amplitude of bursts of beta oscillations (beta bursts)

We defined the length of a burst of beta band oscillations (beta-burst) as the duration for which instantaneous power in the beta band (15-20Hz) remained above a threshold (β_{th}). β_{th} was the average beta band for an uncorrelated ensemble of Poisson spikes trains with same average firing rate as the neurons in the network. Because neurons in our model had different average firing rate (averaged over 5 trials) depending on the external input and network activity states, β_{th} for each network activity state was different. The beta burst amplitude was estimated as the peak power in the beta band. To estimate the beta burst amplitude we smoothened the power spectrum using a cubic kernel. We also estimated the intra-burst frequency which is the peak frequency in β band at the instant when the instantaneous power was above the threshold.

Estimation of excitation-inhibition balance

The E-I balance a GPe neuron was calculated as the ratio of effective excitatory input it received from the STN neurons (J_{EI-eff}) and effective inhibitory input it received from other GPe neurons (J_{II-eff}). The effective synaptic weights J_{EI-eff} , J_{II-eff} were estimated as:

$$J_{EI-eff} = R_{stn} \times J_{stn-gpe} \times \epsilon_{stn-gpe} \times N_{stn} \times \tau_{exc}$$

where R_{stn} is the average firing rate of the STN neurons, $J_{stn-gpe}$ is the synaptic strength of STN→GPe connection, $\epsilon_{stn-gpe}$ is the probability connection from STN to GPe, N_{stn} is the number of STN neuron and τ_{exc} is the time constant of the excitatory synapses (**Table 1**). Similarly, the J_{II-eff} was estimated as:

$$J_{II-eff} = R_{gpe} \times J_{gpe-gpe} \times \epsilon_{gpe-gpe} \times N_{gpe} \times \tau_{inh}$$

where R_{gpe} is the average firing rate of the GPe neurons, $J_{gpe-gpe}$ is the synaptic strength of GPe→GPe connection, $\epsilon_{gpe-gpe}$ is the probability connection from GPe to GPe, N_{stn} is the number of GPe neuron and τ_{inh} is the time constant of the inhibitory synapse (**Table 1**).

Simulation and Data Analysis Tools

The dynamics of STN-GPe network was simulated using NEST (version 2.12.0) [38] with a simulation resolution of 0.1 ms. The SSB neuron model was added to NEST and the code as well as instructions on recompilation will be provided on github. Spiking activity of the network was analyzed using custom code written using SciPy and NumPy libraries. Visualizations were done using Matplotlib [40].

Results

Beta band (15-30 Hz) oscillations in the LFP are a characteristic feature of the neuronal activity in PD patients. Animal models have shown that the emergence of β band oscillations is also accompanied by a change in the firing rate and spike bursting in both STN and GPe neurons. To understand the role of firing rate changes and spike bursting in STN and GPe neurons on the power and duration of β band oscillations we studied the dynamics of the STN-GPe networks by systematically and independently varying the input firing rate and spike bursting of STN and GPe neurons.

STN firing rate determines the strength of β band oscillations

First, we studied the effect of STN and GPe firing rates on the emergence of oscillations. To this end, we systematically varied the rate of external input to STN and GPe neurons and measured the spectral entropy of the population activity to characterize the oscillations (Figure. 2). As expected the GPe firing rates monotonically increased as we increased excitatory input to the STN (Figure. 2A). However, GPe firing rate varied in a non-monotonic fashion as we increased excitatory input to the GPe neurons (Figure. 2A), because of the recurrent inhibition within the GPe. By contrast, STN firing rates monotonically increased as we increased the excitatory input to STN and monotonically decreased as we increased excitatory input to GPe (Figure 2B).

Irrespective of the differences in their mean firing rate, both STN and GPe showed the same oscillation dynamics. More specifically, an increase in the excitatory input to STN or decrease in the excitation to GPe led to the emergence of β band oscillations in the STN-GPe network (Figure. 2C,D - lighter color represents an oscillatory regime). This is consistent with previous studies which showed that increase in excitatory inputs to STN and inhibition to GPe from upstream brain areas are enough to trigger oscillations in the sub-thalamo-pallidal circuitry [24, 28].

These results (Figure 2A-D) also revealed how the β band oscillations depend on the firing rate of the STN and GPe neurons. To better visualize this relationship we rendered spectral entropy the network activity as a function of STN and GPe firing rates (Figure. 2E). We found that GPe firing rates are not predictive of the oscillations in the network. For instance, even if GPe firing rate is kept constant, an increase in firing rate of STN neurons was sufficient to induce oscillations. Similarly, a decrease in STN activity reduced oscillations provided GPe firing rates did not vary. On the other hand, when STN firing rate was low (below 5 Hz), any change in the GPe firing rate was not able to induce oscillations. This can also be observed in a scatter plot of spectral entropy against the STN and GPe firing rates (Figure Supplement ??).

Experimental data [6, 12] as well as previous computational models [24, 26] have suggested that emergence of β band oscillations is accompanied by a decrease in the firing rate of GPe neurons and an increase in the firing rate of STN neurons. Our results suggest that only the STN firing rates are positively correlated with the power of β band oscillations. Based on these observations we argue that a decrease in GPe activity may be necessary but not sufficient condition to induce Parkinsonism. That is, reduction in the firing rate of GPe neurons or lesions of GPe are not sufficient to induce beta band oscillations. This suggestion is consistent the experimental findings that GPe lesions in non-MPTP monkeys do not induce any discernible motor signs of PD [10].

State dependent effect of bursting neurons on β band oscillations

Effect of bursting in GPe neurons on β band oscillations

Besides changes in average firing rate, dopamine depleted animals also show an increase in spike bursting, in both STN and GPe [2, 34]. Thus far it is not clear whether and how spike bursts affect the β band oscillations. In both reduced or biophysical neuron models introduction of spike bursting necessarily affects the total spike rate of the neuron. As we have shown in the previous section firing rate itself has an effect on the oscillations. That is, such neuron models cannot be used to extract the contribution of spike bursting on oscillations. Therefore, we used the SSBN model which allows us to introduce spike bursting in a neuron without affecting its average firing rate [37]. Using this model we systematically altered the fraction of bursting neurons in the STN (FB_{STN}) and GPe (FB_{GPe}). Previously, in a model of neocortical networks we showed

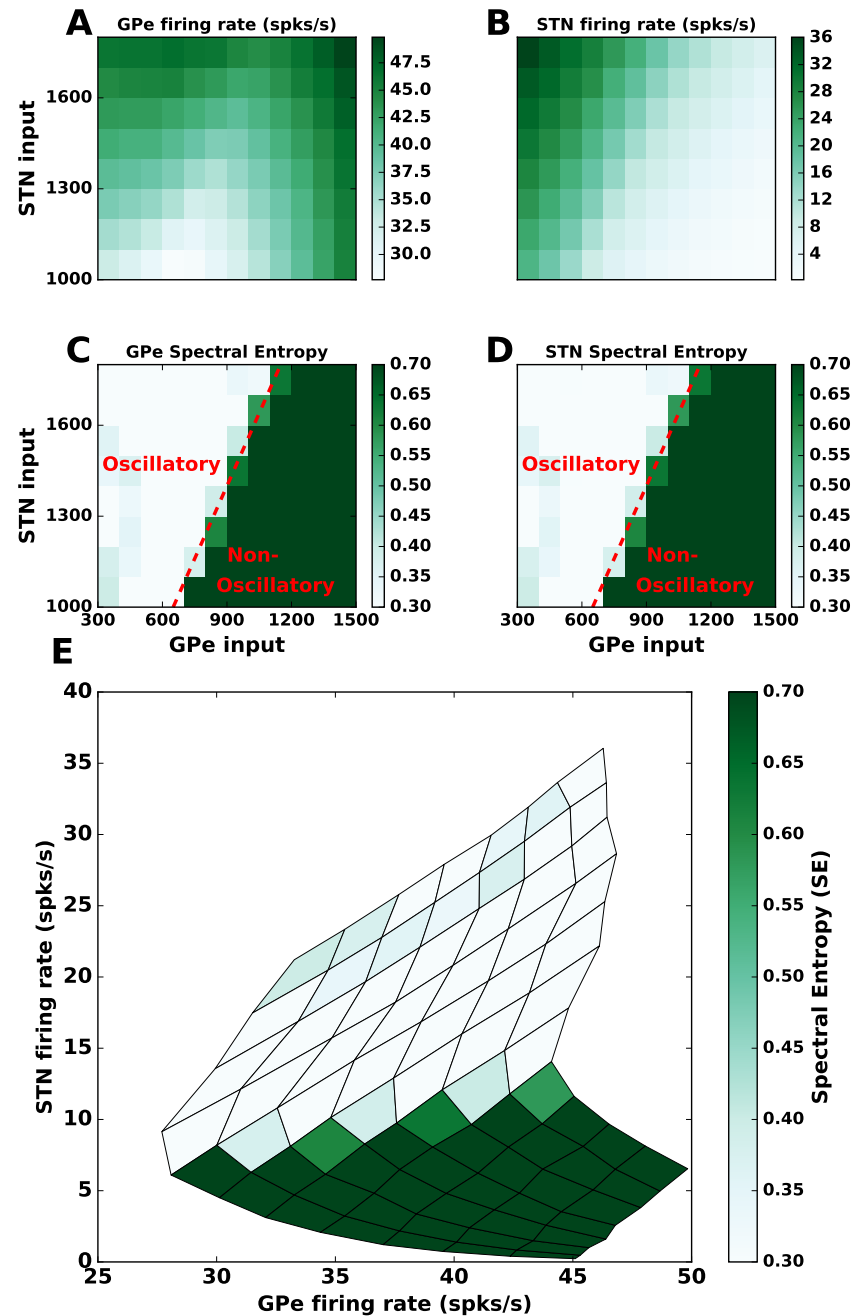


Fig 2. Increased input to STN or decreased input to GPe induces oscillations. (A) Average firing rate of GPe neurons as a function of different input rates to the STN and GPe. (B) Same as in A but for STN neurons. (C) Strength of oscillations in the GPe population (quantified using spectral entropy, see Methods). (D) Same as in C but for STN neurons. (E) The effect of the STN and GPe firing rates (as in A and B) on spectral entropy (as in C and D). These results show that β oscillations in the STN-GPe network depend on the STN firing rate but not on the GPe firing rates. All the values (firing rate and spectral entropy) were averaged over 5 trials. A scatter plot for spectral entropy against the STN and GPe firing rates for all the 5 trials is shown in Figure supplement ??.

that the effect of spike bursting depends on the network activity states [37]. Therefore, we studied the effect of spike bursting on three exemplary network regimes (1) a strong oscillatory regime, (2) at the bifurcation between oscillatory and non-oscillatory regimes and (3) a non-oscillatory regime (marked as 1, 2 and 3 in Fig 3A).

We found that when network was in a strong oscillatory regime (1), an increase in the fraction of bursting neurons in GPe (FB_{GPe}) while altered the average firing rates (Fig 3B - upper panel) had no qualitative effect on the population oscillations (Fig 3B - lower panel). Similarly, when the network was in a non-oscillatory regime (network activity regime 3), FB_{GPe} had no effect on the spike rates and spectrum of the population activity (Figure 3D). That is, in strong oscillatory and completely non-oscillatory states, spike bursting has no consequence for the population activity dynamics.

However, when the network was in a regime close to the border of oscillatory and non-oscillatory regimes (network activity regime 2), increase in FB_{GPe} increased oscillations (Figure 3C - lower panel). This activity regime was characterized by weak oscillations when all neurons are non-bursty, but an introduction of bursting in $\geq 20\%$ GPe neurons (Figure 3C - lower panel). In this network state, an increase in the number of bursting neurons also increased the average population firing rate (Figure 3C - upper panel) in both STN and GPe. Clearly, this increase in firing rates is a network phenomenon induced by bursting and not because of a change in the input excitation (as was shown in Figure 2) or change in the excitability of individual neurons. Finally, an increase in FB_{GPe} increased the network oscillations irrespective of the fraction of bursting neurons in the STN (Figure 3C - lower panel).

Effect of bursting in STN neurons on β band oscillations

In contrast to the bursting in GPe neurons, the effect of spike bursting in STN neurons was not only dependent on the network state but also on the fraction of spike bursting neurons in the GPe. Similar to the effect of spike bursting in GPe neurons, in strong oscillatory and non-oscillatory states a change in the fraction of bursting neurons in the STN population had no effect on the network activity state (Figure 3B,D, Figure supplements ?? and ??).

However, at the border of oscillatory and non-oscillatory regimes of network activity states (network activity regime 2) spike bursts in the STN affect the oscillations in a non-monotonic fashion. As shown above in this regime an increase in fraction of bursty neurons in GPe pushes the network state towards oscillations. We found that in this regime, the impact of STN spike bursting on oscillations depended on FB_{GPe} . For small FB_{GPe} , the network remained in a non-oscillatory state and a change in FB_{STN} had no effect on the spectrum of network activity. Similarly, for high FB_{GPe} , the network remained in an oscillatory state and a change in FB_{STN} had no effect on the spectrum population activity.

At a moderate fraction of spike bursting neurons in GPe ($0.2 < FB_{GPe} < 0.6$), when the network showed weak oscillations, a small increase in the FB_{STN} reduced oscillations ($FB_{STN} < 0.6$ - Figure 3C; Figure supplement ??) but a large increase in FB_{STN} ($geq 0.6$) enhanced oscillations (Figure 3C). That is, there is a range of parameters for which oscillations enhanced by FB_{GPe} can be quenched by increasing FB_{STN} . As FB_{GPe} increases, more FB_{STN} is required to quench the oscillations and as our results show, beyond a certain point increasing FB_{STN} also leads to persistent oscillations. That is, bursting in the STN can suppress or enhance oscillations depending on the fraction of bursting neurons in the GPe.

The non-monotonic effect of STN bursting on STN-GPe network oscillation can be better observed in a spectrogram (Figure 4). As a fraction of GPe neurons ($FB_{GPe}=40\%$ in this case) were changed to elicit spike bursts (at 1500 ms) β band oscillations

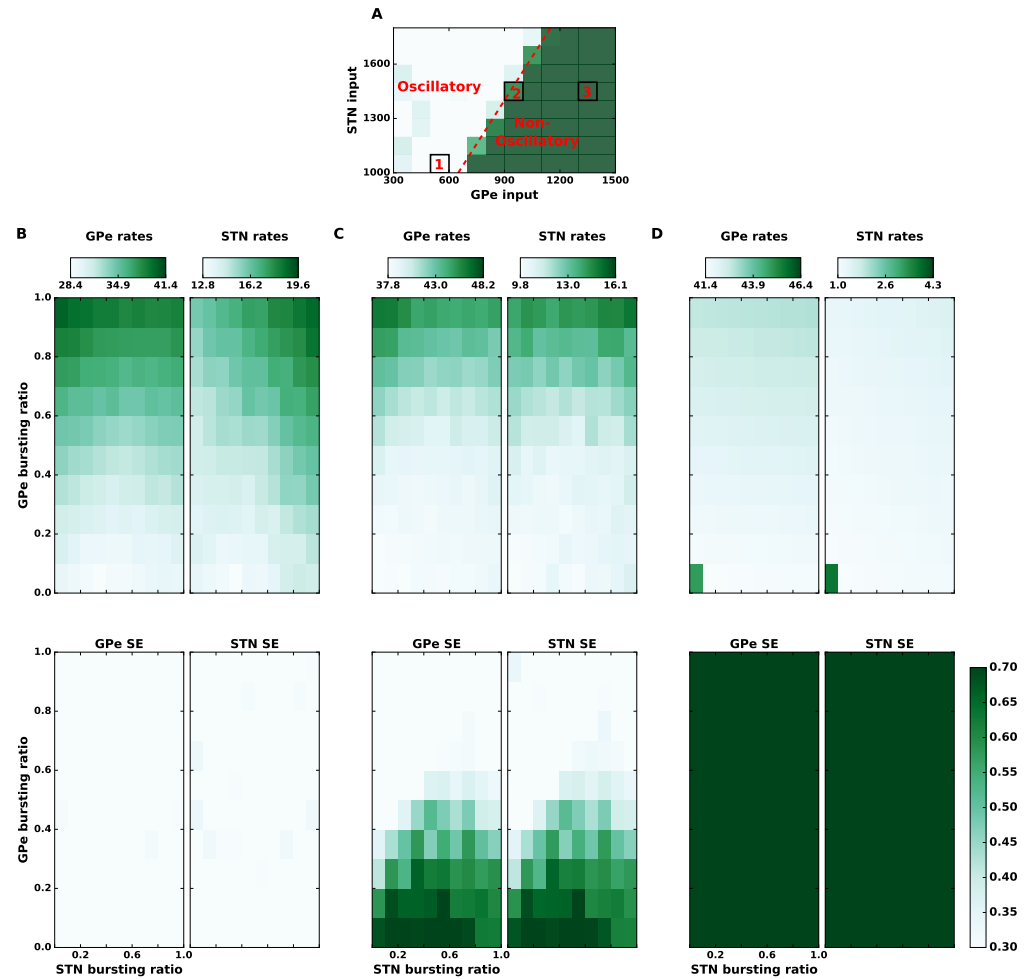


Fig 3. State dependent effect of spike bursting on the strength of β oscillations. (A) Spectral entropy as a function of input to the STN and GPe neurons. This panel is same as the Figure 2C with three regimes of network activity marked, **1**: oscillatory, **2**: regime at the border of oscillatory and non-oscillatory regime, **3**: non-oscillatory regime. (B):**Top** GPe (left) and STN (right) firing rate as a function of the fraction of bursting neurons in the STN (x-axis) and GPe (y-axis), in the oscillatory regime 1. (B):**Bottom** GPe (left) and STN (right) spectral entropy as a function of the fraction of bursting neurons in the STN (x-axis) and GPe (y-axis), in the oscillatory regime (i.e. state 1 in the panel A). Spike bursting has no effect on the network activity dynamics in this regime. (C) Same as in the panel (B) but when the network was operating in a regime at the border of oscillatory and non-oscillatory regimes (i.e. state 2 in the panel A). In this regime, spike bursting affects the network activity state: increase in the fraction of bursting neurons in GPe induces oscillations whereas an optimal fraction of bursting neurons in STN can quench oscillations. (D):**Top** Corresponds to regime 3. Same as (B):**Top**. Addition of BS neurons do not affect a strong non-oscillatory regime. (D):**Bottom** Same as in the panel (B):**Bottom** but when the network was operating a non-oscillatory regime (i.e. state 3 in the panel A). In this regime spike bursting has no effect on network oscillations.

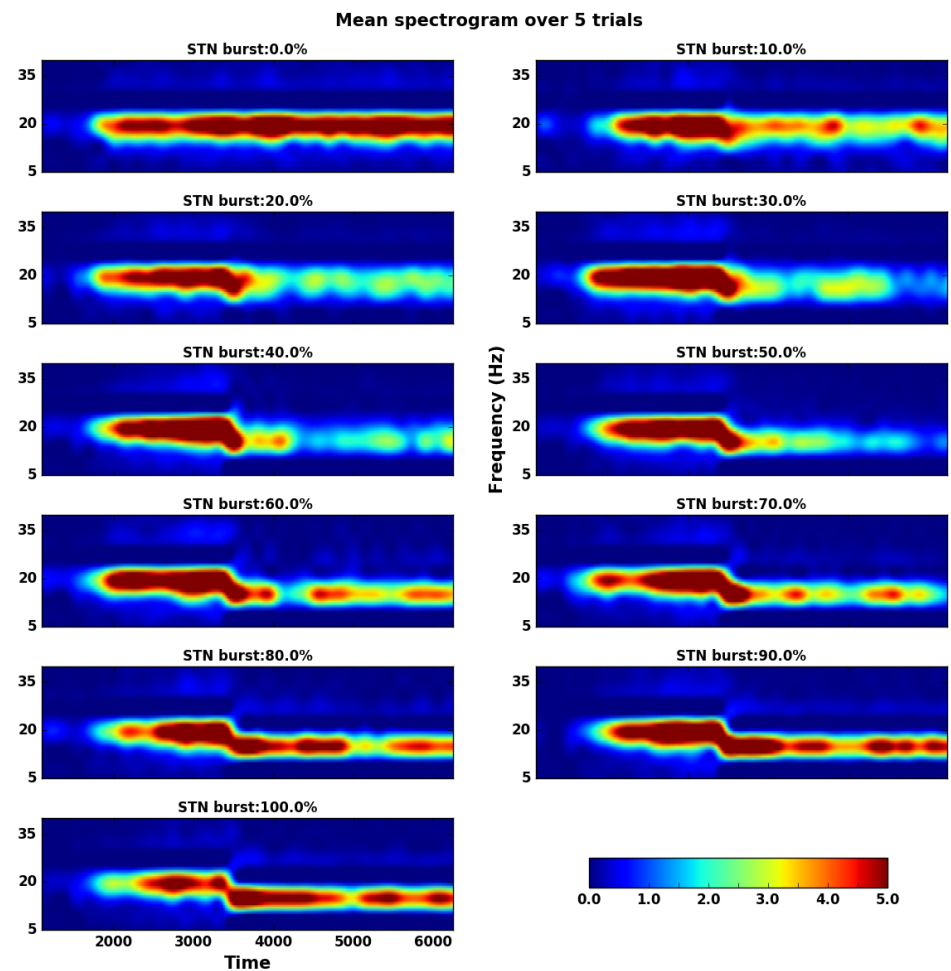


Fig 4. Non-monotonic effect of STN bursting on network oscillations when the network operates close to the border between oscillatory and non-oscillatory states (i.e. state 2 in Fig. 3A. Here the fraction of bursting neurons in the GPe was fixed to 40% of GPe neurons and the fraction of bursting neurons in the STN (FB_{STN}) was increased systematically (as marked on different subplots). 40% of GPe neurons were made to elicit spike bursts from time point 1500 ms. This resulted in emergence of oscillations. A fraction of STN neurons (FB_{STN} marked on each subplot) were made to bursty, starting at time 3500ms. For small to moderate FB_{STN} , oscillations disappeared. But when FB_{STN} was larger oscillations reappeared albeit at a lower frequency. The spectrograms shown here were averaged over 5 trials of the network with different random seeds.

emerged (Figure 4). These oscillations were quenched when STN neurons also started to spike in bursts from time 3500 ms. When $\approx 50\%$ of STN neurons were bursty, the oscillations were almost completely quenched. Any further increase in FB_{STN} , however, led to re-emergence of oscillations, albeit at lower frequencies ($\approx 15\text{Hz}$).

Why does FB_{STN} has a non-monotonic effect on the STN-GPe oscillations? The spectrograms of the network activity (Figure 4) revealed that bursting in GPe and STN induces oscillations at slightly different frequencies. When $FB_{GPe} = 40\%$ and $FB_{STN} = 0$, the network oscillates at $\approx 20\text{Hz}$ (1st panel of Figure 4). By contrast, when $FB_{GPe} = 40\%$ and $FB_{STN} = 100\%$, the network oscillates $\approx 15\text{Hz}$ (last panel of Figure 4). We hypothesized that the interference of these two oscillations may underlie the non-monotonic effect of spike bursting in STN on β band oscillations. For small values of FB_{STN} , the two oscillations interfere and generate network activity resembling ‘beats’, which are reflected as short bursts of β band oscillations. It was these short β oscillations epochs that resulted in a decrease in overall power in the beta-band (and higher spectral entropy). However, for higher FB_{STN} , slower frequency oscillations (generated by STN bursting) become strong enough to overcome the GPe bursting induced oscillations. To verify our hypothesis we imposed a lower frequency (15Hz) oscillation on a fraction of STN neurons instead of making them bursting. As we increased the fraction of neurons that oscillated at 15Hz we observed non-monotonic change in the network oscillation power (Figure Supplement ??). These results are qualitatively similar to those observed when we varied the fraction of bursting neurons in the STN (Figure 4), thus providing support to our hypothesis.

Our results show that when the network is operating close the border of oscillatory and non-oscillatory states (network activity regime 2), change in the fraction of bursting neurons can control the emergence of β oscillations. It is interesting to note that in this regime, the firing rate of STN and GPe neurons falls within the range recorded experimentally (that is, $37\text{--}48\text{ spks/s}$ for GPe, $9\text{--}16\text{ spks/s}$ for STN) for healthy conditions. This also suggests that in healthy states, GPe-STN network may be operating in the regime at the border of oscillatory and non-oscillatory state. In this regime, spike bursting may provide an additional mechanism to generate short lived β band oscillations as has been observed in healthy animals [41], that is, an increase in spike bursting in the GPe can induce oscillations, which can be quenched provided STN neurons also elicit spikes in bursts.

Control of the amplitude and duration of β band oscillation bursts by spike bursts

Next, we explored how the proportion of GPe and STN bursting neurons affects the amplitude and duration of β oscillation bursts. In particular we were interested in identifying the fraction of bursting neurons needed to obtain beta bursts similar to those recorded in the BG during healthy conditions. The length of a β burst was defined as the duration that the beta band amplitude envelope remained above the threshold (Figure 5A). The β threshold (Figure 5A,B) was defined as the averaged maximum (over 5 trials) of the amplitude spectrum of a Poisson process of the same firing rate as that of our network activity. An increase in the fraction of bursting neuron in the GPe increased the average beta burst length. However, an increase in the STN bursting ratio had a non-monotonic effect on the beta burst length as we expected given the effect of FB_{STN} on spectral entropy (Figure. 3C). The beta burst amplitude, however, increased with an increase in fraction of bursting neuron in both GPe and STN (Figure 5D).

To compare the model output with the experimental data we measured three features of the network activity for all combinations of FB_{STN} and FB_{GPe} : average burst length, average intra-burst frequency, and correlation between burst length and burst

amplitude. The average β burst length measured in healthy mice is ≈ 0.2 s [42]. The burst length and burst amplitude in humans [13] as well as non-human primates [43] positively correlated that is, stronger bursts also last longer.

According to these measures, the regime with a small fraction of bursty neurons in GPe (e.g. 10%) and STN (e.g. 20%) (Figure 5C,D - cyan marker) resembled most closely with the experimentally measured values of all the aforementioned features. In this regime, the intraburst frequency was ≈ 20 Hz. Moreover, burst amplitude and burst length (mean value: ≈ 0.24 s) were positively correlated ($r_{bl,ba} = 0.46$, $p \leq 0.0002$) (Figure 5E).

For a higher fraction of bursting neurons in GPe (40%) and STN (40% - Figure 5F), the average burst lengths increases to ≈ 0.8 s, the intraburst frequency decreases to ≈ 16 Hz and the positive correlation between burst amplitude and burst length is high and significant ($r_{bl,ba} = 0.92$, $p < 0.0001$). For the regime with a lower fraction of bursty neurons for GPe (10%) and a higher fraction of bursting neurons in STN (80%), the positive correlation between burst length and burst amplitude was not significant, however the burst length is slightly higher (≈ 0.4 s) and intraburst frequency is slower (≈ 15 Hz).

We, therefore, predict that short lived beta burst in healthy mice are generated when $\approx 10\%$ of GPe neurons and $\approx 20\%$ of STN neurons elicit spike bursts.

Dependence of the network states on the excitation and inhibition balance

Finally, to better understand the impact of firing rate changes and bursting neurons on the β band oscillations we analyzed the balance of effective excitation and inhibition (E-I balance) in the network for different input firing rates and fractions of bursting neurons. E-I balance is the primary determinant of oscillations in spiking neuronal networks [32]. To get an estimate of the E-I balance for a GPe neuron we measured effective excitation it received from a STN neuron (J_{EI-eff}) and effective inhibition it received from other GPe neurons (J_{II-eff}). We estimated the effective excitation and inhibition for all combinations of external input as shown in Figure 2 (See Methods).

Consistent with the previous theoretical work on neuronal network dynamics we found that the non-oscillatory states emerged when effective inhibition received by a GPe neuron was much higher than the effective excitatory inputs, whereas oscillatory states appeared when the effective excitation from STN to a GPe neuron increases (Figure 6).

Next we mapped the effect of GPe and STN spike bursting on the E-I balance in the three exemplary network states (1: oscillatory, 2: border of oscillatory and non-oscillatory, 3: non-oscillatory). As expected we found that in the oscillatory state 1, increase in GPe bursting increased the effective inhibition and excitation whereas STN bursting has a non-monotonic effect (Figure. 6 - state marked as 1). However, in this state bursting in either population was not strong enough to change the E-I balance in order to introduce a qualitative change in the network state. Similarly for the non-oscillatory state 3, a change in the fraction of bursting neuron in the GPe and STN bursting was not sufficient to introduce any qualitative change in the state of the network (Figure 6). When the network was in the regime 2, even though increase in fraction of bursting neuron in the GPe introduced a small change in the effective E-I balance, it was sufficient to move the network activity into the oscillatory regime from non-oscillatory regime. Increased in the fraction of bursting neuron in the STN showed a non-monotonic effect on the E-I balance and while a moderate amount of FB_{STN} pushed the network towards the non-oscillatory regime, which was not the case for a higher FB_{STN} (Figure 6).

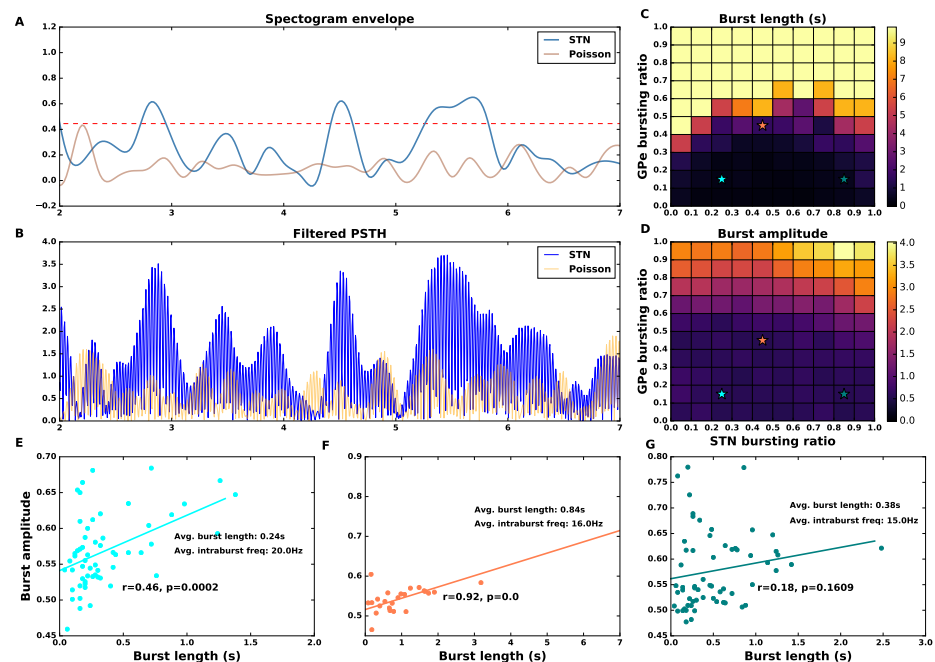


Fig 5. Effect of spike bursting on beta-band oscillation bursts. (A) An example of the amplitude envelope of the beta band (15-20 Hz) oscillations (blue trace). Beta oscillation burst threshold (red dashed line) was determined by averaging the maximum of beta band amplitude envelope for a Poisson process (orange trace) with the same firing rate as the neuron in the STN-GPe network. The averaging was done over Poissonian firing rates corresponding to all GPe and STN bursting ratios and 5 trials per STN-GPe bursty ratio combination. (B) Low pass filtered (15-20 Hz band) trace of population firing rate in the STN population in the beta band (15-20Hz). The orange trace shows the population firing rate of the Poisson process with same average firing rate as the STN activity. (C) Beta oscillation burst length as a function of the fraction of bursting neurons in the GPe and the STN. (D) Beta oscillation burst amplitude as a function of the fraction of bursting neurons in the GPe and the STN. (E,F,G) Correlation between β oscillation burst length and amplitude for three different combinations of FB_{STN} and FB_{GPe} (marker with cyan, orange and green colors in the pane C. Cyan marker shows beta oscillation burst length and amplitude for 10% of bursting neurons in GPe and 20% in STN - this combination of bursting neurons gives an average burst length of 0.24s which is comparable to experimentally measured values. In panels E-F the p-values are listed to 4 places after decimal point.

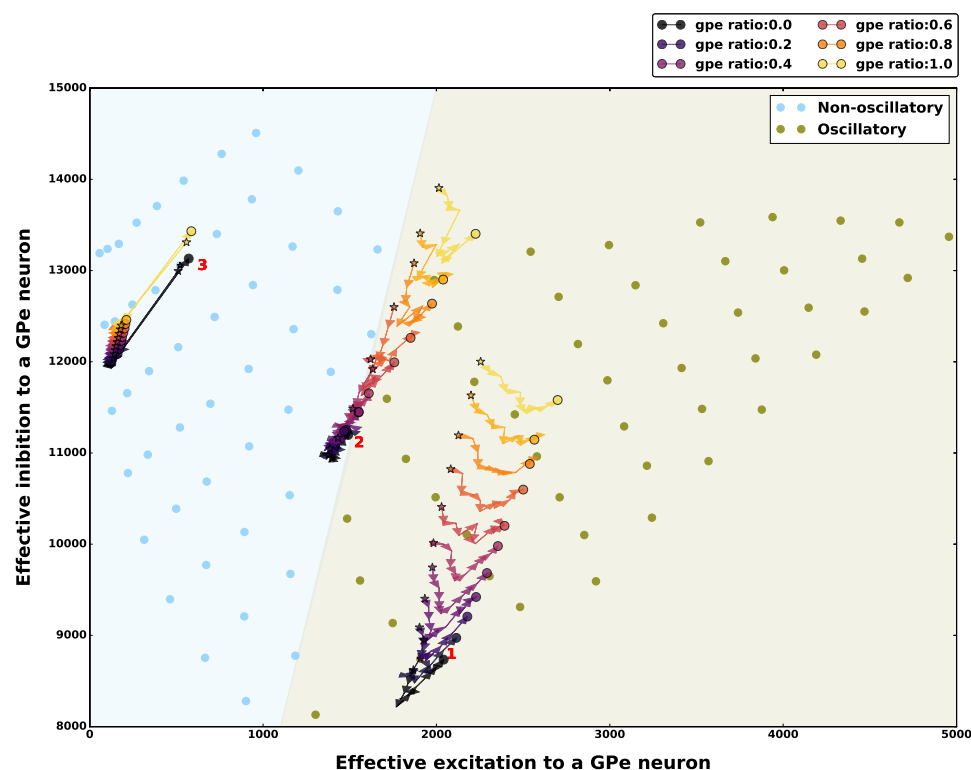


Fig 6. Effect of spike bursting on the excitation-inhibition balance in different network regimes. E-I balance was characterized by estimating the total effective excitation and inhibition received by a GPe neuron (see Methods). E-I balance for oscillatory and non-oscillatory network states for 100% non-bursting neurons. Each filled circle shows E-I balance for different external inputs to STN and GPe neurons shown in Figures 2-3. The effect of spike bursting on E-I balance is shown for the three exemplary network activity regimes: 1-Oscillatory regime, 2-Border of oscillatory and no-oscillatory regime, 3-Non-oscillatory regime (see Figure 3 for details). Different colored stars and filled circles show how the E-I balance varied as function of change in the fraction of bursting neurons in the GPe (warmer colors indicate higher % of bursting neurons). The trajectory from the star (STN bursting ratio = 0%) to the filled circle shows change in the E-I balance as the fraction of bursting in STN is varied from 0% to 100%. In all the states spike bursting tends to make the network activity more oscillatory, however, the amount by which spike bursting is able to push the network towards oscillatory regime depends on the network activity regime itself.

Discussion

PD is characterized by change in both firing rate and firing patterns of GPe and STN as shown in animals models [2, 34–36]. In this study, we focused on uncoupling the roles of STN and GPe population firing rate and firing patterns (bursting) in determining the presence of oscillations. Our results show that an increase in the firing rate of STN neurons is the primary determinant of oscillations in the STN-GPe network, however the effect of changes in GPe firing rates is contingent on the firing rate of STN neurons. Similarly, the effect of increase in spike bursting in STN and GPe neurons is contingent on the dynamical state of the network.

Effect of firing rate changes on β band oscillations

In our model network, an increase in the firing rate of STN neurons was sufficient to drive the network into an oscillatory state, irrespective of the firing rate of the GPe neurons. By contrast, a decrease in the firing rate of GPe neurons was able to generate β band oscillations only when STN neuron firing rate also increased (Figure. 2E, Figure Supplement ??). A change in GPe and STN firing rates also alter the effective excitation-inhibition of the network (Figure 6, 7). The non-oscillatory network states were observed in the inhibition dominant regime (when effective inhibition to a GPe neuron was higher than effective excitation). An increase in effective excitation altered the regime to oscillatory. This result may explain the experimental observation that the therapeutic effect of DBS is accompanied by a corresponding decrease in STN firing rates [?] and an associated corresponding increase in GPe/GPi firing rates [44–46].

Our results also show that if the firing rate of STN neurons remains fixed, changes in the firing rate of GPe neurons are not sufficient to influence the oscillations. Indeed, it can be argued that because STN and GPe are recurrently connected, their firing rates cannot independently change. However, these results imply that the β oscillations are more sensitive to changes in STN firing rates than to GPe firing rates. In our model there are two possible mechanisms to induce beta-band oscillations: (a) The *indirect pathway induced* oscillations can be initiated by reducing the firing rate of GPe neurons via transient increase in firing rate of D2- spiny projection neurons. (b) The *hyper-direct pathway induced* oscillations can be initiated by a transient increase in the firing rate of cortical neurons projecting onto the STN neurons. Our results suggest that the *indirect pathway induced* oscillations can be quenched by transiently decreasing the activity of STN neurons but the *hyper-direct pathway induced* oscillations cannot be countered by transiently increase the activity of GPe neurons.

At the behavioral level, the sensitivity of β band oscillations to STN firing rates could provide an explanation for the importance of STN in response inhibition in general and, especially when there is an increase in potential responses (high conflict task). Experimental data have shown that the STN firing rates increase in proportion to the degree of conflict in an action-selection task [47]. Interestingly, the increase in STN firing rates during a high conflict task is also accompanied by an increase in beta band activity [48] and is reminiscent of increase in STN activity [49] as well as power of the β band oscillations as observed in successful STOP trials [50]. Furthermore, the latency [50] as well as amount of modulation [51] in STN β band oscillations are correlated with the speed of an action. All these observations suggest there may be a functional rationale to the sensitivity of oscillations to STN firing rates as shown by our results. That is, an increase in STN firing rates could be a mechanism to delay the decision making (“hold the horses” [52]) by increasing the β band activity, which cannot be vetoed by the GPe and thereby plays a vital role at response inhibition [53]. This insight might also substantiate the efficacy of DBS in STN as a target nucleus.

Effect of changes in spike bursting on beta band oscillations

Our results show that the effect of GPe or STN bursting is dependent on the state of the network as defined by the firing rates of the STN and GPe neurons. In a regime with strong oscillations, GPe and STN bursting does not qualitatively change the network state and the network remains oscillatory. Similarly, in a non-oscillatory regime, GPe and STN bursting has no qualitative effect on the network state. However, in a regime at the border of oscillatory and non-oscillatory, an increase in bursting neurons in the GPe induces oscillations but the effect of increasing STN bursting neurons depends on the fraction of GPe bursting neurons. In this regime, when bursting neurons in the GPe induce oscillations ($0.1 \leq \text{FB}_{\text{GPe}} \leq 0.4$), a small increase in the fraction of bursting neurons in the STN disrupts the oscillations. However, a large fraction of bursting neurons in the STN re-instate the β band oscillation (Figure 4). This non-monotonic effect of bursting neurons in the STN is because when neurons spike in bursts both STN and GPe tend to induce oscillations at slightly different frequencies (Figure 4, Supplementary Figure ??). The relative power of these oscillations depends on the fraction of bursting neurons in the two populations. When $\text{FB}_{\text{GPe}} = \text{FB}_{\text{STN}} \approx 0.5$ the magnitude of the two oscillations is comparable and they produce ‘beats’ resulting in a reduction in the power of beta band oscillations. However, if $\text{FB}_{\text{GPe}} \geq 0.5$ or $\text{FB}_{\text{STN}} \geq 0.5$, the stronger of the two oscillations overcomes the other, resulting in the higher power in the β band.

Similar to the rate effect, the effect of spike bursting can also be captured by calculating the balance of effective excitation and inhibition in the network (Figure 6, 7). GPe bursting increases both the effective excitation and inhibition to a GPe neuron. Therefore, when a network is operating close to the border of oscillatory and non-oscillatory regime, increase in bursting in GPe neurons pushes the network to an oscillatory regime (Figure 7). An increase in bursting neurons in the STN, however, has a non-monotonic effect – a smaller number of bursting neurons counter the effect of GPe bursting by decreasing both effective excitation and inhibition. However the effect of larger number of STN neurons bursting collude with the effect of GPe bursting by increasing both effective excitation and inhibition (Figure 7).

During PD, both STN and GPe neuron show an increase in bursting activity [2, 34–36]. Based on our results, we propose that increase in STN bursting might play a compensatory role in an attempt to quench the burst induced oscillations. This might also explain the observation that STN stimulation using deep brain stimulation is only therapeutic in the range where the STN neurons respond intermittently to stimulation with bursts (135-180Hz, 90-200 μ secs stimulation, [54]).

Tandem of GPe-STN bursting generates bursts of beta oscillations

In healthy conditions, short epochs of oscillations (beta bursts) have been observed in rodents [42] and non-human primates [43]. They are also observed in Parkinsonian patients during dopamine ON state [13]. The precise function of beta bursts in healthy conditions is currently unknown but they tend to occur before movement (e.g after the cue [41]) and disappear when the movement is initiated [55–58]. Beta bursts become longer and stronger during Parkinsonian conditions [13], therefore, they are thought to be correlated with impairment of voluntary movement in PD patients. The average length of the beta bursts in healthy rodents last for an average of 0.2 sec [42]. In our model, we can generate the oscillatory β bursts of average burst length 0.24 s by making 10% of GPe and 20% of STN neurons are of spike bursting type (Figure 5). We propose that an interplay of spike bursts in GPe and STN may be the underlying mechanism to generate short bursts of beta oscillations.

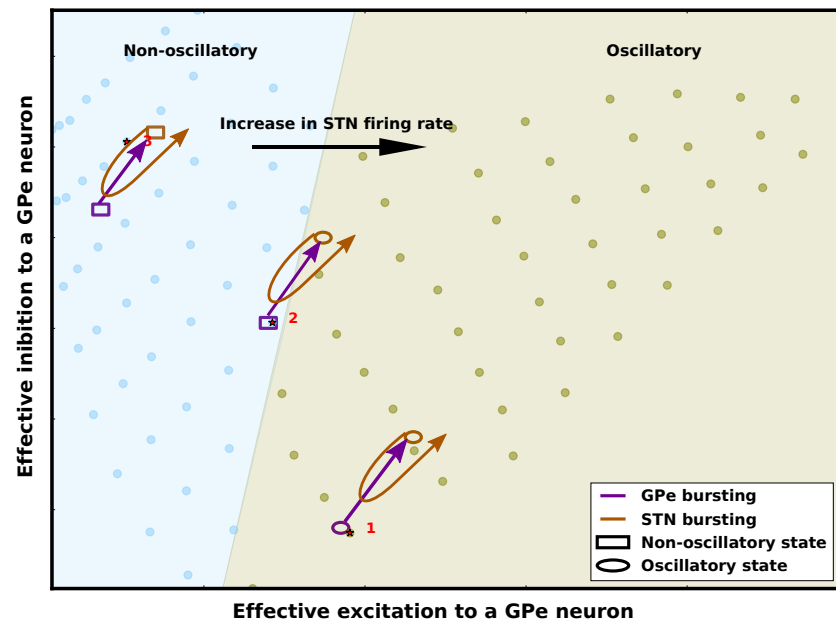


Fig 7. Summary of the effect of firing rate and spike bursting on network state. The background image (copied from the Figure 6) show the oscillatory and non-oscillatory regimes of STN-GPe network as a function of effective excitation and inhibition. The arrows schematically show the change in EI-balances as we increase spike bursting in the STN or GPe. The STN-GPe network oscillations are more sensitive to the STN firing rate. The balance of STN and GPe firing rates determines the global state of network activity. Spike bursting in GPe always increases both effective inhibition and effective excitation. Small increases in spike bursting in STN results in a decrease in both effective excitation and effective inhibition and thereby, reduces oscillations. By contrast, a large increase in the fraction of bursting neurons in the STN increases both effective inhibition and effective excitation and thereby, enhances oscillations. However, this effect is smaller and therefore, spike bursting is effective in altering the network oscillations only when the network is operating close to the border of oscillatory and non-oscillatory states.

Experimental results have shown that an increased bursting in STN is associated with an increase in hyperpolarization of the neuron's membrane potential [59]. That is, spike bursts in the GPe network (e.g. because of striatal bursts [60]) can induce spike bursting in the STN neuron by inducing large synchronized inhibition. However, if only less than 50% of the GPe neurons generate spike bursts, an equivalent proportion of neurons bursting in STN will quench the oscillations resulting in a short-lived “beta burst”.

However, in pathological conditions, the network state could be pushed into the oscillatory regime (either due to a change in firing rates or excessive bursting) where these oscillations can no longer be quenched. This has been explained in the summary figure 7.

Our results also suggest that in healthy conditions the network might operate on the boundary of synchronization and asynchronization regime. Operating at the boundary enables the network to make incursions into the oscillatory regime (when GPe neurons

elicit spike bursts) and retreat to the asynchronization regime (when STN neurons elicit spike bursts) with a proportion of bursting neurons where such self-regulated transitions are possible. However, in pathological conditions, the network very likely shifts deeper into the oscillation regime (due to the change in firing rates or excessive bursting), where no amount of STN bursting can push the network back to asynchronized regime.

Operating on the boundary could have many advantages such as easy creation and dissolution of transient neuronal assemblies [61] as required by functioning of network shown in other parts of basal ganglia (especially striatum, [62–66]). *Rubchinsky et. al* also suggested that a Parkinsonian network might also operate on the boundary albeit with a bias towards a state with increased synchrony.

We also suggest a novel functional role for bursting neurons in GPe and STN in healthy conditions as a mechanism to generate these short-lived beta bursts. However, the same mechanism leads to runaway oscillations when the network is no longer on the boundary but is shifted deeper into the oscillatory regime.

These new insights about the role of spike rates, spike bursts and varied roles of STN and GPe in shaping of the dynamics of beta band oscillations suggest several means of quenching the pathological oscillations for instance by (1) reducing the firing rate of the STN neurons, (2) reducing the excitability of STN neurons, and (3) by balancing the fraction of bursting and non-bursting neurons in the STN and GPe.

Acknowledgments

We thank Drs. Arthur Leblois and Robert Schmidt for their input on the work. This work was funded by the Swedish Research Council (StratNeuro and India-Sweden collaboration grant and VR research project grant) and German Research Foundation (DFG; grant DI 1721/3-1 [KFO219-TP9]), the Helmholtz Association through the Helmholtz Portfolio Theme "Supercomputing and Modeling for the Human Brain" (SMHB), Initiative and Networking Fund of the Helmholtz Association and Ger-Jpn Comput Neurosci Project, German Federal Ministry for Education and Research (BMBF Grant 01GQ1343).

References

1. Mallet N, Ballion B, Le Moine C, Gonon F. Cortical inputs and GABA interneurons imbalance projection neurons in the striatum of parkinsonian rats. *The Journal of neuroscience : the official journal of the Society for Neuroscience*. 2006;26(14):3875–84. doi:10.1523/JNEUROSCI.4439-05.2006.
2. Tachibana Y, Iwamuro H, Kita H, Takada M, Nambu A. Subthalamo-pallidal interactions underlying parkinsonian neuronal oscillations in the primate basal ganglia. *Eur J Neurosci*. 2011;34(9):1470–1484.
3. Sharott A, Vinciati F, Nakamura KC, Magill PJ. A population of indirect pathway striatal projection neurons is selectively entrained to parkinsonian beta oscillations. *Journal of Neuroscience*. 2017;doi:10.1523/JNEUROSCI.0658-17.2017.
4. Hammond C, Bergman H, Brown P. Pathological synchronization in Parkinson's disease: networks, models and treatments. *Trends in neurosciences*. 2007;30(7):357–64. doi:10.1016/j.tins.2007.05.004.
5. Costa RM, Lin SC, Sotnikova T, Cyr M, Gainetdinov R, Caron M, et al. Rapid Alterations in Corticostriatal Ensemble Coordination during Acute

- Dopamine-Dependent Motor Dysfunction. *Neuron*. 2006;52(2):359–369.
doi:10.1016/j.neuron.2006.07.030.
6. Raz A, Vaadia E, Bergman H. Firing Patterns and Correlations of Spontaneous Discharge of Pallidal Neurons in the Normal and the Tremulous 1-Methyl-4-Phenyl-1,2,3,6-Tetrahydropyridine Vervet Model of Parkinsonism. *The Journal of neuroscience : the official journal of the Society for Neuroscience*. 2000;20(22):8559–8571.
7. Mallet N, Pogosyan A, Márton LF, Bolam JP, Brown P, Magill PJ. Parkinsonian beta oscillations in the external globus pallidus and their relationship with subthalamic nucleus activity. *The Journal of neuroscience : the official journal of the Society for Neuroscience*. 2008;28(52):14245–58.
doi:10.1523/JNEUROSCI.4199-08.2008.
8. Levy R, Hutchison WD, Lozano AM, Dostrovsky JO. Synchronized neuronal discharge in the basal ganglia of parkinsonian patients is limited to oscillatory activity. *J Neurosci*. 2002;22(7):2855–2861.
9. Sharott A, Magill PJ, Bolam JP, Brown P. Directional analysis of coherent oscillatory field potentials in the cerebral cortex and basal ganglia of the rat. *Journal of Physiology*. 2005;562(3):951–963. doi:10.1113/jphysiol.2004.073189.
10. Soares J, Kliem MA, Betarbet R, Greenamyre JT, Yamamoto B, Wichmann T. Role of external pallidal segment in primate parkinsonism: Comparison of the effects of 1-Methyl-4-Phenyl-1,2,3,6-Tetrahydropyridine-Induced parkinsonism and lesions of the external pallidal segment. *Neurobiology of Disease*. 2004;24(29):6417–6426. doi:10.1523/JNEUROSCI.0836-04.2004.
11. Brown P, Oliviero A, Mazzone P, Insola A, Tonali P, Di Lazzaro V. Dopamine dependency of oscillations between subthalamic nucleus and pallidum in Parkinson's disease. *J Neurosci*. 2001;21(3):1033–1038.
12. Bergman H, Wichmann T, Karmon B, DeLong MR. The primate subthalamic nucleus. II. Neuronal activity in the MPTP model of parkinsonism. *J Neurophysiol*. 1994;72(2):507–520.
13. Tinkhauser G, Pogosyan A, Tan H, Herz DM, Kühn AA, Brown P. Beta burst dynamics in Parkinson's disease off and on dopaminergic medication. *Brain*. 2017;140(11):2968–2981. doi:10.1093/brain/awx252.
14. Tass P, Smirnov D, Karavaev A, Barnikol U, Barnikol T, Adamchik I, et al. The causal relationship between subcortical local field potential oscillations and Parkinsonian resting tremor. *J Neural Eng*. 2010;7(1):16009.
15. Timmermann L, Wojtecki L, Gross J, Lehrke R, Voges J, Maarouf M, et al. Ten-hertz stimulation of subthalamic nucleus deteriorates motor symptoms in Parkinson's disease. *Movement Disorders*. 2004;19(11):1328–1333.
doi:10.1002/mds.20198.
16. West TO, Berthouze L, Halliday DM, Litvak V, Sharott A, Magill PJ, et al. Propagation of beta/gamma rhythms in the cortico-basal ganglia circuits of the parkinsonian rat. *Journal of Neurophysiology*. 2018;119(5):1608–1628.
doi:10.1152/jn.00629.2017.

17. Roopun AK, Middleton SJ, Cunningham MO, LeBeau FEN, Bibbig A, Whittington MA, et al. A beta2-frequency (20-30 Hz) oscillation in nonsynaptic networks of somatosensory cortex. *Proceedings of the National Academy of Sciences*. 2006;103(42):15646–15650. doi:10.1073/pnas.0607443103.
18. Yamawaki N, Stanford IM, Hall SD, Woodhall GL. Pharmacologically induced and stimulus evoked rhythmic neuronal oscillatory activity in the primary motor cortex in vitro. *Neuroscience*. 2008;151(2):386–395. doi:10.1016/j.neuroscience.2007.10.021.
19. Sharott A, Gulberti A, Hamel W, Köppen JA, Münchau A, Buhmann C, et al. Spatio-temporal dynamics of cortical drive to human subthalamic nucleus neurons in Parkinson's disease. *Neurobiology of Disease*. 2018;112(November 2017):49–62. doi:10.1016/j.nbd.2018.01.001.
20. McCarthy MM, Moore-Kochlacs C, Gu X, Boyden ES, Han X, Kopell N. Striatal origin of the pathologic beta oscillations in Parkinson's disease. *Proc Natl Acad Sci USA*. 2011;108(28):11620–11625.
21. Corbit VL, Whalen TC, Zitelli KT, Crilly SY, Rubin JE, Gittis aH. Pallidostriatal Projections Promote Oscillations in a Dopamine-Depleted Biophysical Network Model. *Journal of Neuroscience*. 2016;36(20):5556–5571. doi:10.1523/JNEUROSCI.0339-16.2016.
22. Plenz D, Kital ST. A basal ganglia pacemaker formed by the subthalamic nucleus and external globus pallidus. *Nature*. 1999;400(6745):677–682.
23. Terman D, Rubin JE, Yew AC, Wilson CJ. Activity Patterns in a Model for the Subthalamopallidal Network of the Basal Ganglia . *J Neurosci*. 2002; p. 2963–2976.
24. Kumar A, Cardanobile S, Rotter S, Aertsen A. The Role of Inhibition in Generating and Controlling Parkinson's Disease Oscillations in the Basal Ganglia. *Front Syst Neurosci*. 2011;5.
25. Rubin JE, McIntyre CC, Turner RS, Wichmann T. Basal ganglia activity patterns in parkinsonism and computational modeling of their downstream effects. *Eur J Neurosci*. 2012;36(2):2213–2228.
26. Holgado AJN, Terry JR, Bogacz R. Conditions for the generation of beta oscillations in the subthalamic nucleus-globus pallidus network. *J Neurosci*. 2010;30(37):12340–12352.
27. Pavlides A, Hogan SJ, Bogacz R. Computational Models Describing Possible Mechanisms for Generation of Excessive Beta Oscillations in Parkinson's Disease. 2015; p. 1–29. doi:10.1371/journal.pcbi.1004609.
28. Mirzaei A, Kumar A, Leventhal D, Mallet N, Aertsen A, Berke J, et al. Sensorimotor Processing in the Basal Ganglia Leads to Transient Beta Oscillations during Behavior. *Journal of Neuroscience*. 2017;37(46):11220–11232. doi:10.1523/JNEUROSCI.1289-17.2017.
29. Stein E, Bar-Gad I. Beta oscillations in the cortico-basal ganglia loop during parkinsonism. *Experimental Neurology*. 2013;245:52–59. doi:10.1016/j.expneurol.2012.07.023.

30. Chen CC, Litvak V, Gilbertson T, Kühn A, Lu CS, Lee ST, et al. Excessive synchronization of basal ganglia neurons at 20 Hz slows movement in Parkinson's disease. *Experimental Neurology*. 2007;205(1):214–221. doi:10.1016/j.expneurol.2007.01.027.
31. Gradinaru V, Mogri M, Thompson KR, Henderson JM, Deisseroth K. Optical deconstruction of parkinsonian neural circuitry. *Science (New York, NY)*. 2009;324(5925):354–9. doi:10.1126/science.1167093.
32. Ledoux E, Brunel N. Dynamics of Networks of Excitatory and Inhibitory Neurons in Response to Time-Dependent Inputs. *Frontiers in Computational Neuroscience*. 2011;5(May):1–17. doi:10.3389/fncom.2011.00025.
33. Leblois A, Boraud T, Meissner W, Bergman H, Hansel D. Competition between feedback loops underlies normal and pathological dynamics in the basal ganglia. *The Journal of neuroscience : the official journal of the Society for Neuroscience*. 2006;26(13):3567–83. doi:10.1523/JNEUROSCI.5050-05.2006.
34. Wichmann T, Soares J. Neuronal firing before and after burst discharges in the monkey basal ganglia is predictably patterned in the normal state and altered in parkinsonism. *J Neurophysiol*. 2006;95(4):2120–2133.
35. Vila M, Périer C, Féger J, Yelnik J, Faucheux B, Ruberg M, et al. Evolution of changes in neuronal activity in the subthalamic nucleus of rats with unilateral lesion of the substantia nigra assessed by metabolic and electrophysiological measurements. *European Journal of Neuroscience*. 2000;12(1):337–344. doi:10.1046/j.1460-9568.2000.00901.x.
36. Breit S, Bouali-Benazzouz R, Popa RC, Gasser T, Benabid AL, Benazzouz A. Effects of 6-hydroxydopamine-induced severe or partial lesion of the nigrostriatal pathway on the neuronal activity of pallido-subthalamic network in the rat. *Experimental Neurology*. 2007;205(1):36–47. doi:10.1016/j.expneurol.2006.12.016.
37. Sahasranamam A, Vlachos I, Aertsen A, Kumar A. Dynamical state of the network determines the efficacy of single neuron properties in shaping the network activity. *Scientific Reports*. 2016;6(May):1–16. doi:10.1038/srep26029.
38. Kunkel S, Morrison A, Weidel P, Eppler JM, Sinha A, Schenck W, et al.. *NEST* 2.12.0; 2017.
39. Blanco S, Garay A, Coulombie D. Comparison of frequency bands using spectral entropy for epileptic seizure prediction. *ISRN Neurol*. 2013;2013:287327.
40. Hunter JD. Matplotlib: A 2D Graphics Environment. *Comput Sci Eng*. 2007;9(3):90–95.
41. Leventhal DK, Gage GJ, Schmidt R, Pettibone JR, Case AC, Berke JD. Basal ganglia beta oscillations accompany cue utilization. *Neuron*. 2012;73(3):523–536.
42. Bello EP, Casas-Cordero R, Galiñanes GL, Casey E, Belluscio MA, Rodríguez V, et al. Inducible ablation of dopamine D2 receptors in adult mice impairs locomotion, motor skill learning and leads to severe parkinsonism. *Molecular Psychiatry*. 2017;22(4):595–604. doi:10.1038/mp.2016.105.
43. Deffains M, Iskhakova L, Katabi S, Israel Z, Bergman H. Longer Beta Oscillatory Episodes Reliably Identify Pathological Subthalamic Activity in Parkinsonism. *Movement Disorders*. 2018;00(00):1–10. doi:10.1002/mds.27418.

44. Hashimoto T, Elder CM, Okun MS, Patrick SK, Vitek JL. Stimulation of the subthalamic nucleus changes the firing pattern of pallidal neurons. *J Neurosci*. 2003;23(5):1916–1923.
45. Meissner W, Leblois A, Hansel D, Bioulac B, Gross CE, Benazzouz A, et al. Subthalamic high frequency stimulation resets subthalamic firing and reduces abnormal oscillations. *Brain*. 2005;128(Pt 10):2372–2382.
46. Birdno MJ, Grill WM. Mechanisms of deep brain stimulation in movement disorders as revealed by changes in stimulus frequency. *Neurotherapeutics*. 2008;5(1):14–25.
47. Zaghoul Ka, Weidemann CT, Lega BC, Jaggi JL, Baltuch GH, Kahana MJ. Neuronal activity in the human subthalamic nucleus encodes decision conflict during action selection. *The Journal of neuroscience : the official journal of the Society for Neuroscience*. 2012;32(7):2453–60. doi:10.1523/JNEUROSCI.5815-11.2012.
48. Brittain JS, Watkins KE, Joundi Ra, Ray NJ, Holland P, Green AL, et al. A role for the subthalamic nucleus in response inhibition during conflict. *The Journal of neuroscience : the official journal of the Society for Neuroscience*. 2012;32(39):13396–401. doi:10.1523/JNEUROSCI.2259-12.2012.
49. Schmidt R, Leventhal DK, Mallet N, Chen F, Berke JD. Canceling actions involves a race between basal ganglia pathways. *Nature Neuroscience*. 2013;16(8):1118–1124. doi:10.1038/nn.3456.
50. Ray NJ, Jenkinson N, Brittain J, Holland P, Joint C, Nandi D, et al. The role of the subthalamic nucleus in response inhibition: Evidence from deep brain stimulation for Parkinson's disease. *Neuropsychologia*. 2009;47(13):2828–2834. doi:10.1016/j.neuropsychologia.2009.06.011.
51. Herz DM, Tan H, Brittain JS, Fischer P, Cheeran B, Green AL, et al. Distinct mechanisms mediate speed-accuracy adjustments in cortico-subthalamic networks. *eLife*. 2017;6:357–381. doi:10.7554/eLife.21481.
52. Frank MJ, Samanta J, Moustafa Aa, Sherman SJ. Hold your horses: impulsivity, deep brain stimulation, and medication in parkinsonism. *Science (New York, NY)*. 2007;318(5854):1309–12. doi:10.1126/science.1146157.
53. Zavala B, Zaghoul K, Brown P. The subthalamic nucleus, oscillations, and conflict. *Movement Disorders*. 2015;30(3):n/a–n/a. doi:10.1002/mds.26072.
54. Garcia L, D'Alessandro G, Fernagut PO, Bioulac B, Hammond C. Impact of high-frequency stimulation parameters on the pattern of discharge of subthalamic neurons. *J Neurophysiol*. 2005;94(6):3662–3669.
55. Kühn AA, Williams D, Kupsch A, Limousin P, Hariz M, Schneider GH, et al. Event-related beta desynchronization in human subthalamic nucleus correlates with motor performance. *Brain*. 2004;127(Pt 4):735–746.
56. Tan H, Pogosyan A, Anzak A, Ashkan K, Bogdanovic M, Green AL, et al. Complementary roles of different oscillatory activities in the subthalamic nucleus in coding motor effort in Parkinsonism. *Exp Neurol*. 2013;248:187–195.

57. Courtemanche R, Fujii N, Graybiel AM. Synchronous, focally modulated beta-band oscillations characterize local field potential activity in the striatum of awake behaving monkeys. *The Journal of neuroscience : the official journal of the Society for Neuroscience*. 2003;23(37):11741–11752. doi:23/37/11741 [pii].
58. Androulidakis AG, Doyle LMF, Yarrow K, Litvak V, Gilbertson TP, Brown P. Anticipatory changes in beta synchrony in the human corticospinal system and associated improvements in task performance. *European Journal of Neuroscience*. 2007;25(12):3758–3765. doi:10.1111/j.1460-9568.2007.05620.x.
59. Beurrier C, Congar P, Bioulac B, Hammond C. Subthalamic nucleus neurons switch from single-spike activity to burst-firing mode. *J Neurosci*. 1999;19(2):599–609.
60. Cagnan H, Nicolas M, Moll CKE, Gulberti A, Westphal M, Gerloff C, et al. Temporal evolution of beta bursts in the parkinsonian cortico-basal ganglia network. *bioRxiv*. 2018;doi:10.1101/458414.
61. Rubchinsky LL, Park C, Worth RM. Intermittent neural synchronization in Parkinson ' s disease. 2012; p. 329–346. doi:10.1007/s11071-011-0223-z.
62. Humphries MD, Wood R, Gurney K. Dopamine-modulated dynamic cell assemblies generated by the GABAergic striatal microcircuit. *Neural networks : the official journal of the International Neural Network Society*. 2009;22(8):1174–88. doi:10.1016/j.neunet.2009.07.018.
63. Ponzi A, Wickens J. Sequentially switching cell assemblies in random inhibitory networks of spiking neurons in the striatum. *Journal of Neuroscience*. 2010;30(17):5894–5911. doi:10.1523/JNEUROSCI.5540-09.2010.
64. Barbera G, Liang B, Zhang L, Gerfen C, Culurciello E, Chen R, et al. Spatially Compact Neural Clusters in the Dorsal Striatum Encode Locomotion Relevant Information. *Neuron*. 2016;92(1):202–213. doi:10.1016/j.neuron.2016.08.037.
65. Klaus A, Martins GJ, Paixão VB, Zhou P, Paninski L, spatiotemporal organization of the striatum encodes action space Costa RMT. The spatiotemporal organization of the striatum encodes action space. Submitted. 2017;95(5):1171–1180.e7. doi:10.1016/j.neuron.2017.08.015.
66. Spreizer S, Angelhuber M, Bahuguna J, Aertsen A, Kumar A. Activity Dynamics and Signal Representation in a Striatal Network Model with Distance-Dependent Connectivity. *Eneuro*. 2017;4(August):ENEURO.0348–16.2017. doi:10.1523/ENEURO.0348-16.2017.